

Effects of coupled translational-torsional motion and eccentricity between centre of mass and centre of stiffness on wind-excited tall buildings

S. Thepmongkorn[†]

Construction Engineering and Technology Division, Mahanakorn University of Technology, Thailand

K.C.S. Kwok[‡]

*Department of Civil Engineering, Hong Kong University of Science and Technology, Hong Kong and
Department of Civil Engineering, University of Sydney, NSW 2600, Australia*

Abstract. Wind tunnel aeroelastic model tests of the Commonwealth Advisory Aeronautical Research Council (CAARC) standard tall building were conducted using a three-degree-of-freedom base hinged aeroelastic (BHA) model. Experimental investigation into the effects of coupled translational-torsional motion, cross-wind/torsional frequency ratio and eccentricity between centre of mass and centre of stiffness on the wind-induced response characteristics and wind excitation mechanisms was carried out. The wind tunnel test results highlight the significant effects of coupled translational-torsional motion, and eccentricity between centre of mass and centre of stiffness, on both the normalised along-wind and cross-wind acceleration responses for reduced wind velocities ranging from 4 to 20. Coupled translational-torsional motion and eccentricity between centre of mass and centre of stiffness also have significant impacts on the amplitude-dependent effect caused by the vortex resonant process, and the transfer of vibrational energy between the along-wind and cross-wind directions. These resulted in either an increase or decrease of each response component, in particular at reduced wind velocities close to a critical value of 10. In addition, the contribution of vibrational energy from the torsional motion to the cross-wind response of the building model can be greatly amplified by the effect of resonance between the vortex shedding frequency and the torsional natural frequency of the building model.

Key words: coupled motion; complex motion; tall buildings; eccentricity; wind-induced response characteristics; wind excitation mechanisms.

1. Introduction

One of the most important design consideration for modern tall and slender buildings is wind-induced forces and responses, in particular the resultant acceleration response which affects occupant comfort. However, the analysis of wind-induced forces and responses is a complicated process due to the turbulent nature of the upstream wind, flow separations, vortex formations, and aeroelastic effects. As a result, wind tunnel model tests have become an integral part of the design process. The prediction of wind-induced forces and responses of tall buildings with complex

[†] Lecturer

[‡] Professor

geometrical shapes, such as multiple level of set-backs, or buildings with an asymmetrical stiffness distribution in plan, such as the lift core located at the corner, is more complicated due to the effects of coupled translational-torsional motion.

The important effects of coupled translational-torsional motion on wind-induced response characteristics of tall buildings have been recognised by both analytical and experimental studies, e.g., Patrickson and Friedman (1979), Tallin and Ellingwood (1985), Kareem (1985), Yip and Flay (1995), and Yoshie *et al.* (1997). For a comprehensive study of the wind-induced response characteristics and wind excitation mechanisms, the results from wind tunnel aeroelastic model tests and the corresponding detailed analyses, highlighting the significant effects of coupled translational-torsional motion, and eccentricity between centre of mass and centre of stiffness, are presented in this paper. The experimental results previously obtained by Thepmongkorn and Kwok (1998) have been re-analysed in more details to provide a better understanding of the excitation and response processes and these are presented and discussed in the subsequent sections.

2. Experimental programmes

2.1. Three-degree-of-freedom base hinged aeroelastic model

A three-degree-of-freedom base hinged assembly (BHA) technique (Thepmongkorn and Kwok 1998), as shown in Fig. 1, was used in this study. A BHA independently simulates building translational motions using two perpendicular plane frames, denoted as ABCD and KLMN, and torsional motion

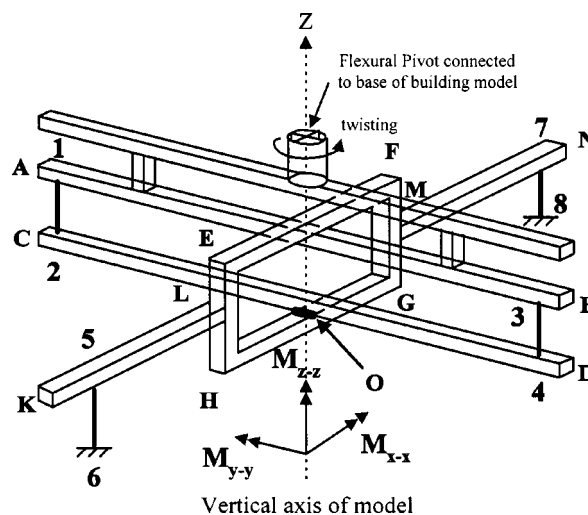


Fig. 1 Three-degree-of-freedom base hinged assembly technique
 AB and CD are rigid members aligned in the same vertical planes.
 EFGH is a rigid rectangular frame, GH is attached to bottom of CD while EF runs above and perpendicular to AB.
 KL and MN are rigid members attached to frame EFGH.
 1-2 and 3-4 are flexural elements designed to measure the overturning moment M_{y-y} .
 5-6 and 7-8 are flexural elements designed to measure the overturning moment M_{x-x} .

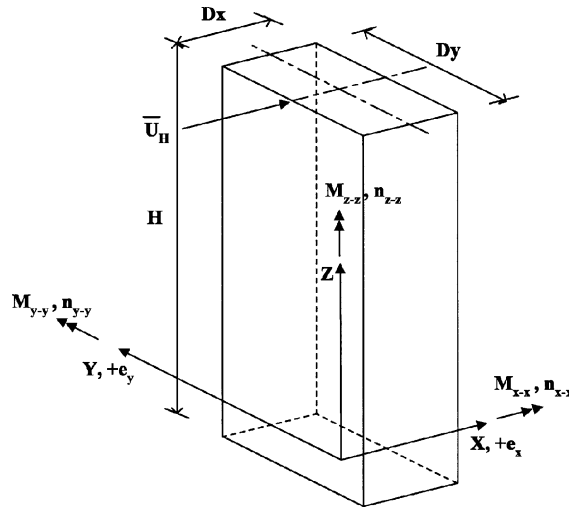


Fig. 2 CAARC standard tall building model and notations

using an additional pivot attached to the top of the BHA. Details of the development of the BHA technique to simulate building motion are discussed by Kwok *et al.* (1994), Thepmongkorn and Kwok (1998), and Thepmongkorn *et al.* (1999).

The rectangular prismatic shape CAARC standard tall building having a full-scale width $D_x = 30$ m, length $D_y = 45$ m, height $H = 180$ m, and structural density $\rho_s = 160$ kg/m³, as shown in Fig. 2, was selected for a detailed study. The subject building has the linear sway mode shapes, rotating about the base of the building model, constant torsional mode shape, and structural damping $\zeta \cong 0.01$ in all modes of vibration. The natural frequencies of the building model were selected as variable parameters for an investigation into the effects of translational/torsional frequency ratios on wind-excited tall buildings. A 1:400 scaled timber model of the CAARC building was attached to a BHA, forming a BHA model.

2.2. Experimental programmes and case studies

Three uni-directional accelerometers were located at top of the building model to investigate the effects of coupled translational-torsional motion and structural eccentricity on wind-induced response characteristics. Two accelerometers were located at points A and B, as shown in Fig. 3, close to the top of the building model, and about 40 mm apart, to measure the accelerations of the building model in the y direction, denoted as \ddot{y}_a and \ddot{y}_b respectively. Another accelerometer was located at point C to measure the acceleration in the x direction, denoted as \ddot{x} . A similar arrangement of accelerometers was found to be a satisfactory method of identifying the effects of torsional motion, i.e., Hart *et al.* (1975) and Yip (1995). In this study, it was assumed that the acceleration caused by torsional motion would manifest itself as translational accelerations when the angle of twist is small. Therefore, the translational acceleration \ddot{x} and \ddot{y}_a were used as an indicator of the wind-induced response characteristics and discussions are based on these two accelerations.

It is noted that the axis of the accelerometer changes its orientation corresponding to the torsional motion of the building model. The acceleration measured by the accelerometers should be converted

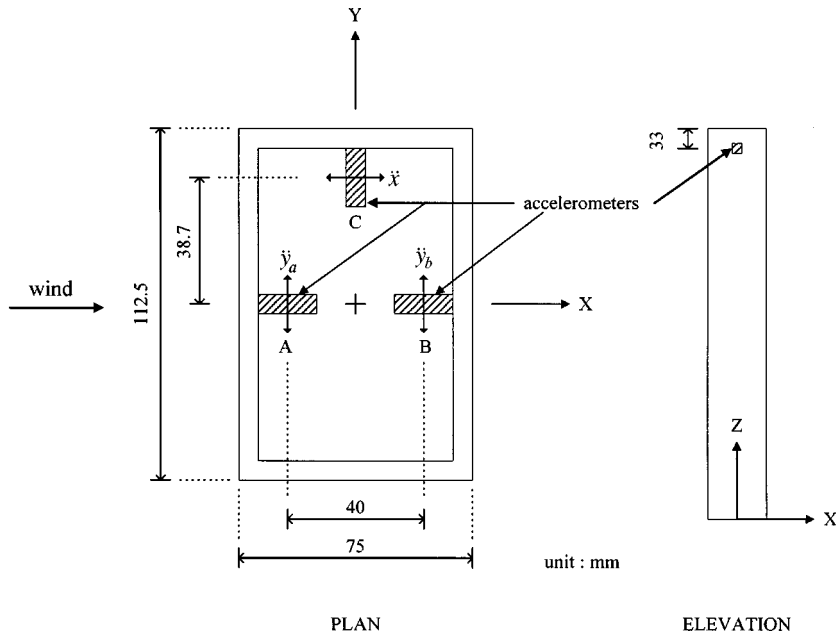


Fig. 3 Arrangements of the accelerometers at top of the building model

to the components of acceleration in the along-wind and cross-wind directions, according to the angle of twist of the building model. However, this effect of change in the orientation of the accelerometer axis on the along-wind and cross-wind acceleration responses was neglected as the observed twisting angle was small, generally smaller than 3° for the incident wind normal to the wide face of the building model. Furthermore, when the angle of twist of the building model was significant, the accelerometer designed to measure the along-wind acceleration would detect a significant contribution from the cross-wind acceleration, and vice versa. However, the cross talk between the acceleration in the along-wind and cross-wind directions on the measured acceleration, in particular the acceleration response spectrum, resulting from change in the orientation of the accelerometer axis was neglected because the twisting angle of the building model was small.

An open terrain wind model, classified as terrain category 2 in AS1170.2-1989 (Standards Australia 1989), with a power law exponent of the mean wind speed profile $\alpha \cong 0.15$ and a turbulence intensity at top of the building model $I_u \cong 0.10$ was simulated. Six test cases as shown in Table 1 were tested in a boundary layer wind tunnel and these were carried out for the incident wind normal to the wide face of the building model.

2.3. Analysis methodology

Results from the analysis of response spectrum, wake spectrum, upcrossing frequency, and correlation between response components are presented to better understand the wind excitation mechanisms. Details of each analysis are summarised below:

- (1) Analysis of response spectrum: provides information on the energy distribution over the range of frequencies interested. A peak in the response spectrum represents a concentrated energy of

Table 1 Experimental test cases for a study of coupled translational-torsional motion of tall buildings

Case	n_{x-x}^* Hz	n_{y-y}^* Hz	n_{z-z}^* Hz	n_{x-x} / n_{z-z}	e_x mm	e_y mm	e_x / D_x %	e_y / D_y %
1	4.04	4.35	∞	-	0	0	0	0
2	3.33	3.96	5.54	0.60	0	0	0	0
3	4.68	3.64	5.54	0.84	0	0	0	0
4	4.68	3.64	5.54	0.84	+10	0	+13.3	0
5	4.68	3.64	5.54	0.84	+10	-10	+13.3	-8.9
6	4.68	3.64	5.54	0.84	0	-10	0	-8.9

* n_{x-x} , n_{y-y} and n_{z-z} listed in the table are natural frequencies of the building model about x , y and z axes respectively, obtained from free vibration tests when it underwent coupled translational-torsional motion.

vibration at a particular frequency. Therefore, the peaks in the spectrum can be used to identify the types of motion, whether they are the along-wind, cross-wind, or torsional motions, and also to estimate the energy contribution from other directions, as well as from other sources such as vortex shedding excitation;

- (2) Analysis of wake spectrum: provides information on the energy contribution in the wake due to the vortex shedding process. Velocity fluctuations in the near wake of the CAARC building model were measured by a linearised DISA hot-wire anemometer, which is the most common type of instrumentation used for investigations of this nature, such as Melbourne (1974) and Saunders (1974). According to Kwok (1977), the hot-wire is best located just outside the wake region to avoid the effect of flow reversals, but close enough to detect the frequency of velocity fluctuations due to the periodic vortex shedding wakes. Therefore, the hot-wire was located at $1.25D$ aside from the outside edge and $2.5D$ downstream from the leading edge of the building model, where D is the afterbody length of the building model, and at a measuring height of approximately 75% of the building height;
- (3) Analysis of upcrossing frequency: provides information on the response processes and the excitation mechanisms. For lightly damped structures oscillating at its natural frequency, the probability distribution of the response is expressed in terms of upcrossings rather than on a time basis. The upcrossing frequency of the response is a measure of the number of upcrossings of the response, on average, above a certain level. According to Melbourne (1977), this level can be conveniently expressed in terms of a reduced variate, which is the number of standard deviations by which the peak value exceeds the mean value. The upcrossing frequency analysis can be used to establish the probability distribution of the response, in particular variations from a normally distributed process;
- (4) Analysis of correlation between response components: provides information on the significance of the torsional motion as well as other excitation mechanisms. The correlation, $\rho[x, y]$, is a measure of the relationship between two variables and is defined by the ratio between the covariance of the two variables and the product of their standard deviation, hence,

$$\rho[x, y] = \frac{\text{Cov}(x, y)}{\sigma_x \sigma_y}, \text{ in which } -1 \leq \rho[x, y] \leq 1. \quad \text{Cov}(x, y) = \frac{1}{n} \sum_{i=1}^n [(x_i - \bar{x})(y_i - \bar{y})] \text{ is}$$

the covariance between the two variables x and y , and the notations \bar{x} , \bar{y} , σ_x , and σ_y represent the mean values and standard deviation values of the variables x and y respectively.

3. Wind-induced response of tall buildings with coupled translational-torsional motion: buildings without eccentricity

Presentations and discussions on the results are based on three categories of reduced wind velocities. Category-one is for reduced wind velocities well below the critical value of 10, hence it is representative of the normal wind speeds for practical applications. Category-two is for reduced wind velocities close to the critical value of 10 and Category-three is for reduced wind velocities higher than the critical value of 10.

With the incident wind normal to the wide face of the building model, the resultant standard deviation accelerations at point C, σ_x , and point A, σ_{y_a} , of the CAARC building model are plotted as a function of reduced wind velocity, $U_r = \bar{U}_H / (n_{x-x} \cdot D_y)$, in Fig. 4. The resultant standard deviation along-wind acceleration, σ_x , was normalised by $(2\pi n_{y-y})^2 D_y$, and the resultant standard deviation cross-wind acceleration, σ_{y_a} , was normalised by $(2\pi n_{x-x})^2 D_y$ as shown in Figs. 4a and 4b respectively. It is noted that the same reduced wind velocity, $U_r = \bar{U}_H / (n_{x-x} \cdot D_y)$, was applied to both Figs. 4a and 4b to better understand a transfer of vibrational energy between the along-wind and cross-wind directions for a particular wind speed tested. Since the cross-wind oscillation is generally higher than the along-wind vibration, the reduced wind velocity was normalised by the cross-wind natural frequency, to correlate the operating reduced wind velocity with the Strouhal number, which significantly affects the cross-wind responses of tall buildings. Case 1 is representative of a tall rectangular building with two translational degree-of-freedom, which is also the case where torsional motion is normally neglected for conventional wind tunnel aeroelastic model studies. Case 2 is

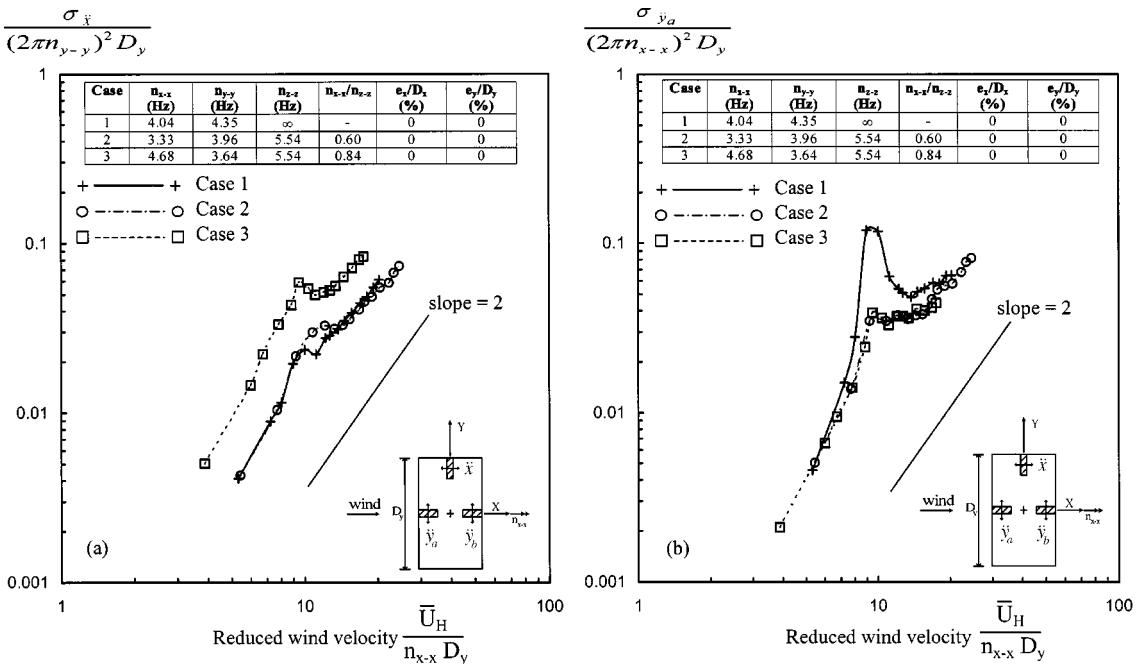


Fig. 4 Normalised resultant standard deviation acceleration responses at top of the CAARC building model as a function of reduced wind velocity for different cross-wind/torsional frequency ratios: (a) along-wind responses; (b) cross-wind responses

representative of a general tall rectangular building whose torsional natural frequency is well separated from the cross-wind natural frequency, i.e., $n_{x-x}/n_{z-z} = 0.60$, while Case 3 represents a building whose torsional natural frequency is getting close to the cross-wind natural frequency, $n_{x-x}/n_{z-z} = 0.84$. The specific term “resultant acceleration” represents the acceleration which contains both translational components caused by translational motion and torsional motion, due to the eccentricity between the accelerometer locations and the line passing through the centre of twist of the building model.

3.1. Resultant along-wind and cross-wind acceleration responses of the CAARC building model for reduced wind velocities ranging from 4 to 8

Coupled translational-torsional motion has a negligible effect on the normalised resultant standard deviation along-wind response for Case 2, but increases the response for Case 3 by 150%, as shown in Fig. 4a. The increase in the normalised along-wind response for Case 3 is consistent with an enhanced transfer of vibrational energy from the cross-wind direction through the torsional motion

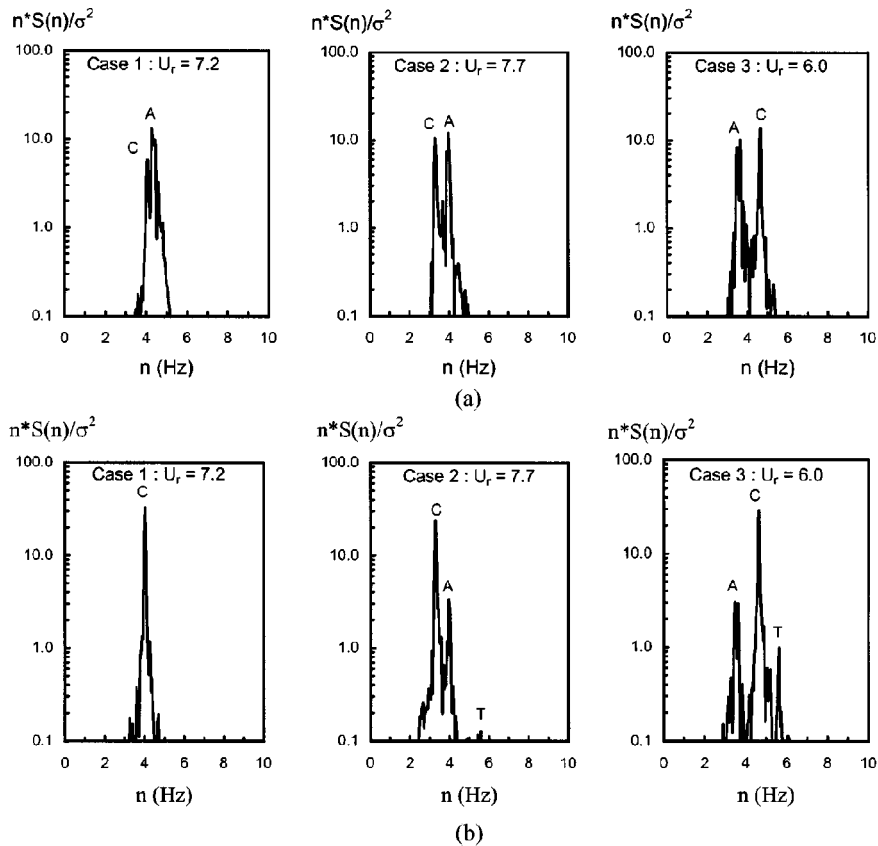


Fig. 5 Acceleration response spectra of the CAARC building model for reduced wind velocities ranging from 4 to 8 for different cross-wind/torsional frequency ratios: (a) along-wind responses; (b) cross-wind responses

of the building model as the frequencies of vibration in cross-wind and torsional directions approach each other. This is confirmed by the results from the analysis of response spectrum shown in Fig. 5a, which indicated an enhanced contribution of vibrational energy from the cross-wind motion for Case 3 as seen by the highest peak at the cross-wind natural frequency compared with other cases.

The decreases in the normalised resultant standard deviation cross-wind responses of the CAARC building model for Case 2 and Case 3 due to coupled translational-torsional motion are evident, as shown in Fig. 4b. These effects of coupled translational-torsional motion were found to be independent of the cross-wind/torsional frequency ratio. The results also indicate a greater decrease in the normalised cross-wind response as reduced wind velocity increases, with a reduction by up to 50% at reduced wind velocities close to 8. It is believed that the decrease in the normalised cross-wind response for both cases of cross-wind/torsional frequency ratios was caused by an increase in the inertia force of the building model when it underwent coupled translational-torsional motion. This is consistent with the results from the analysis of response spectrum, which indicated a significant contribution of vibrational energy from the along-wind motion for both Cases 2 and 3 as shown in Fig. 5b. A contribution of vibrational energy from the torsional motion for Case 3 is more evident as the cross-wind/torsional frequency ratio of the building model approaches unity.

The results from the analysis of upcrossing frequency suggested that the response process for both the along-wind and cross-wind directions is a near normal process for all cases, including the case for tall buildings with coupled translational-torsional motion. This is due to the incident turbulence excitation mechanism in the along-wind direction and the wake excitation mechanism in the cross-wind direction.

3.2. Resultant along-wind and cross-wind acceleration responses of the CAARC building model for reduced wind velocities ranging from 8 to 12

As shown in Fig. 4a, a considerable increase in the normalised resultant standard deviation along-wind response by 150% was observed for Case 3, while a slight increase in the normalised resultant standard deviation along-wind response was observed for Case 2. In addition, there is a peak in the normalised along-wind response for both Cases 2 and 3 at reduced wind velocities close to a critical value of 10. This is believed to be caused by an enhanced transfer of vibrational energy from the cross-wind direction through torsional motion of the building model. Furthermore, a more prominent response peak is evident for Case 3, which is consistent with an enhanced transfer of energy when the frequencies of vibration in the cross-wind and torsional directions approach each other. This is confirmed by the results from the analysis of response spectrum shown in Fig. 6a, which indicated the highest contribution of vibrational energy from the cross-wind motion for Case 3. However, even with such a significant contribution of vibrational energy from the cross-wind oscillation, it was suggested by the results from the analysis of upcrossing frequency that the response processes in the along-wind direction are essentially normally distributed for all cases of cross-wind/torsional frequency ratios.

It is evident from Fig. 4b that coupled translational-torsional motion has a significant effect on the normalised resultant standard deviation cross-wind responses of tall buildings. A significant reduction in the normalised cross-wind response by approximately 65% at reduced wind velocities close to a critical value of 10 was observed for both Cases 2 and 3. The amplitude-dependent excitation caused by the vortex resonant process, which normally dominates the cross-wind response of the building model for this reduced wind velocity range, was dramatically reduced by the coupled

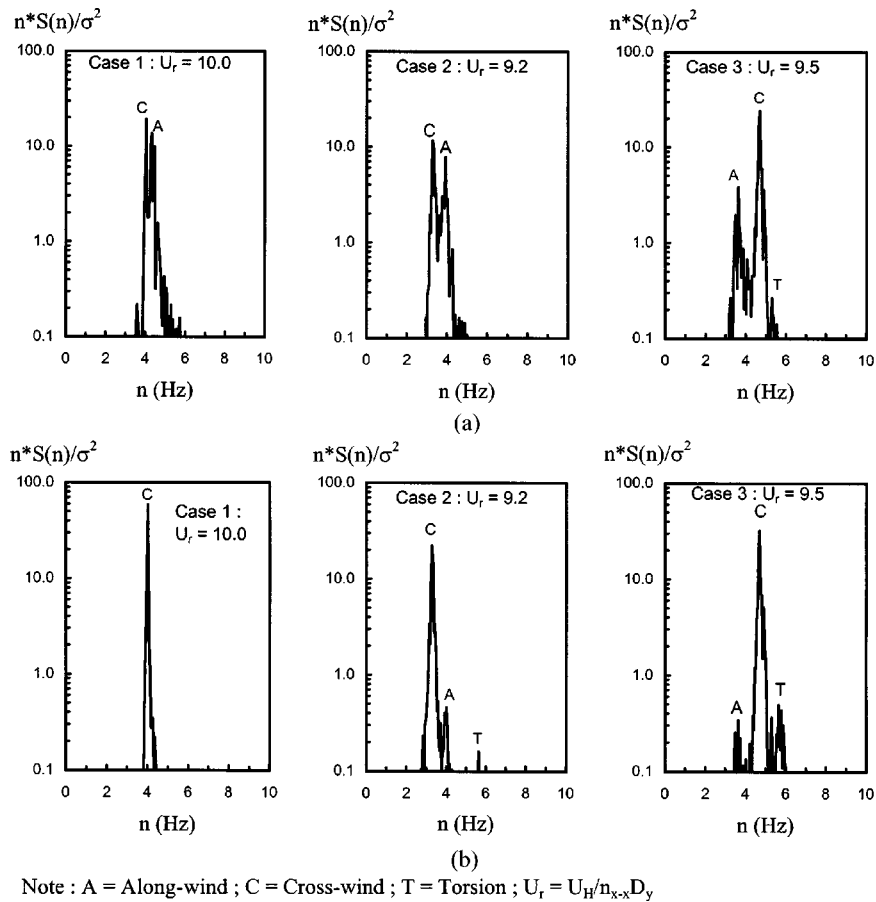


Fig. 6 Acceleration response spectra of the CAARC building model for reduced wind velocities close to a critical value of 10 for different cross-wind/torsional frequency ratios: (a) along-wind responses; (b) cross-wind responses

translational-torsional motion. Furthermore, this effect appears to be independent of the cross-wind/torsional frequency ratio.

The above conclusions can be further supported by the results from the detailed analysis. As shown in Fig. 6b, the cross-wind responses of the building model for all cases are evidently dominated by the cross-wind motion. The spectral peak at the cross-wind natural frequencies for Case 2 and Case 3 are lower than the peak in the response spectrum for Case 1. These correspond to the lower cross-wind responses for both Cases 2 and 3 at reduced wind velocities close to a critical value of 10 as shown in Fig. 4b, due to a significant reduction of the amplitude-dependent effect caused by the vortex resonant process. This is readily illustrated by the results from the analysis of upcrossing frequency shown in Fig. 7 where there is a clear departure of the upcrossing frequency of the response from a normally distributed process for Case 1 due to a significant interdependence between the excitation and response processes or the amplitude-dependent effect. However, for the building model with coupled translational-torsional motion, the amplitude-dependent effect was less prominent as indicated by a smaller departure of the upcrossing frequency

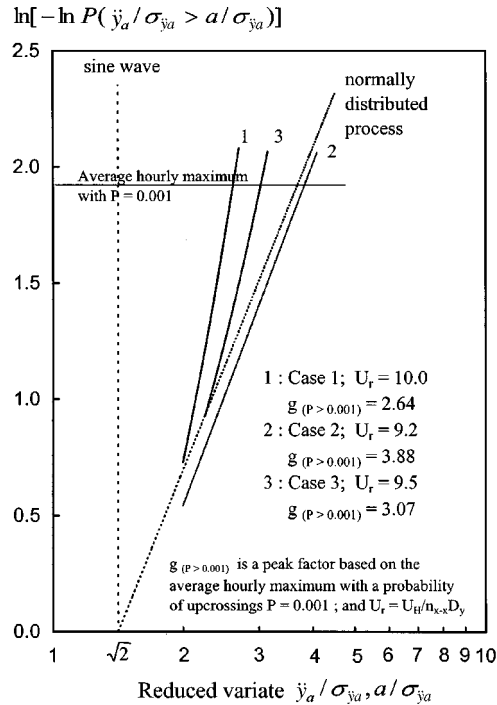


Fig. 7 Normalised upcrossing frequency of the cross-wind responses for the CAARC building model with different cross-wind/torsional frequency ratios for reduced wind velocities close to a critical value of 10

from a normally distributed process for Case 3 and a near normally distributed process for Case 2.

3.3. Resultant along-wind and cross-wind acceleration responses of the CAARC building model for reduced wind velocities higher than 12

Coupled translational-torsional motion considerably increased the normalised resultant standard deviation along-wind response for Case 3 by about 100% but indicated a negligible effect on the normalised along-wind response for Case 2, as shown in Fig. 4a. The results from the analysis of upcrossing frequency further suggested that the along-wind response processes for all cases are approximately normally distributed.

It is evident from Fig. 4b that the normalised resultant standard deviation cross-wind responses for Case 2 and Case 3 are generally lower than the response for Case 1, in which the decreases in the normalised cross-wind responses by approximately 25% were observed. However, for a very high reduced wind velocity range, i.e., for reduced wind velocities higher than 18, the effect of coupled translational-torsional motion appears to be negligible, as the normalised cross-wind responses for both Cases 2 and 3 approach the response for Case 1. The results from the analysis of wake spectrum and response spectrum indicated that the wake excitation and the vortex shedding process remain the dominant excitation mechanisms in the cross-wind direction. However, since the vortex shedding frequency is well removed from the cross-wind natural frequency, the amplitude-dependent effect caused by the vortex resonant process is not evident. Therefore, the cross-wind response process was found to be a near normal distribution for all cases.

3.4. Significance of torsional motion from the analysis of correlation between response components

The correlation between the along-wind and cross-wind acceleration responses, $\rho[\ddot{x}, \ddot{y}_a]$ and the correlation between the cross-wind acceleration responses of the building model at point A and point B, $\rho[\ddot{y}_a, \ddot{y}_b]$, are presented in Figs. 8a and 8b respectively.

For reduced wind velocities ranging from 4 to 8, the correlation $\rho[\ddot{x}, \ddot{y}_a]$ for all test cases tend to increase as the mean wind speed increases, as shown in Fig. 8a. The magnitude of correlation $\rho[\ddot{x}, \ddot{y}_a]$ for Case 2 and Case 3 are generally higher than the correlation for Case 1, which is consistent with a transfer of vibrational energy from cross-wind oscillation to the along-wind direction due to coupled translational-torsional motion. It is noted that the negative values of the correlation $\rho[\ddot{x}, \ddot{y}_a]$ for Case 3 indicate a change in the phase lag between the along-wind and cross-wind motions, compared with the responses for Case 1 and Case 2. This is believed to be caused by the effect of the cross-wind/along-wind frequency ratio of the building model, which changed from below 1.0 for Case 1 and Case 2 to above 1.0 for Case 3. This change in the cross-wind/along-wind frequency ratio created a change in the phase lag between the along-wind and cross-wind motions, hence the negative values of the correlation $\rho[\ddot{x}, \ddot{y}_a]$ for Case 3 as shown in Fig. 8a.

At reduced wind velocities close to a critical value of 10, the peak in the correlation $\rho[\ddot{x}, \ddot{y}_a]$ is evident for all cases. These high correlation between along-wind and cross-wind responses are caused by a transfer of vibrational energy between the two motions. The highest absolute value of correlation of about 0.75 for all cases appears to be independent of the cross-wind/torsional frequency ratio and thus this may represent the maximum value of the correlation $\rho[\ddot{x}, \ddot{y}_a]$ for the CAARC building model with coupled translational-torsional motion. On the other hand, for reduced wind velocities higher than 15, the along-wind and cross-wind responses of the building model for all cases appear to be independent of each other as indicated by the near zero value of the

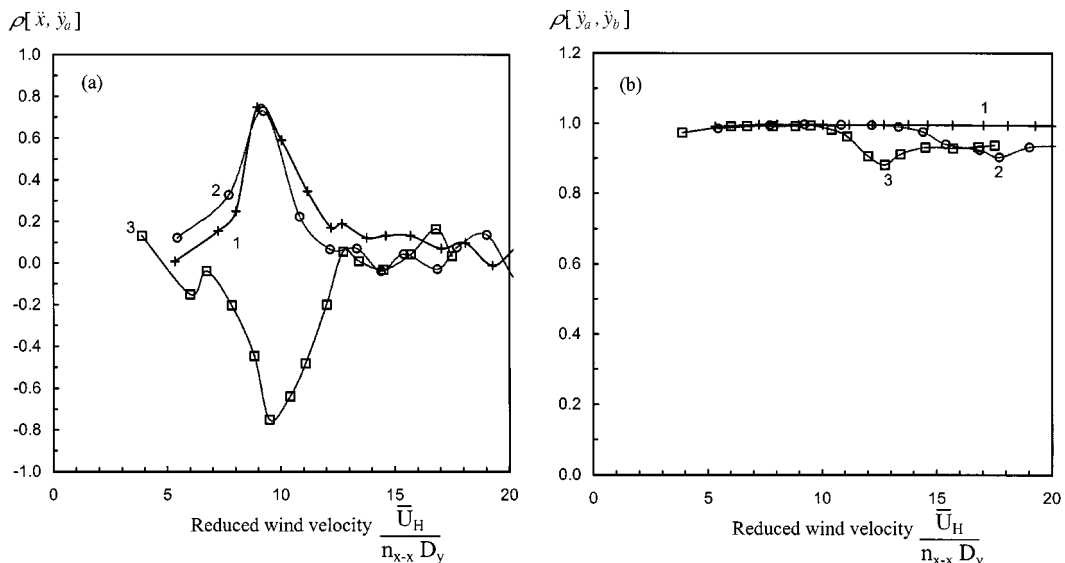


Fig. 8 Correlation between response components: (a) along-wind and cross-wind responses; (b) cross-wind responses at point A and point B

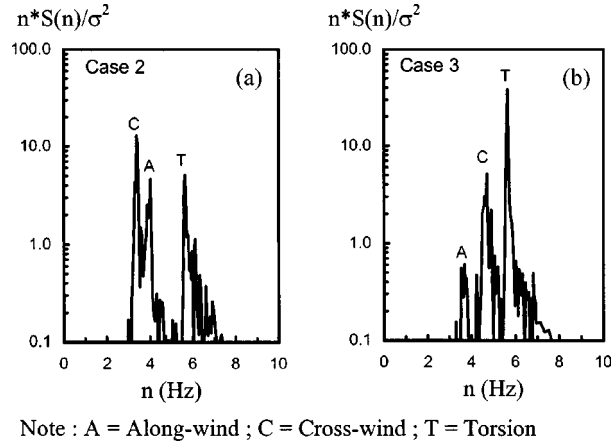


Fig. 9 Cross-wind acceleration response spectra of the CAARC building model at the critical reduced wind velocity for torsional motion for different cross-wind/torsional frequency ratios: (a) cross-wind/torsional frequency ratio of 0.60; (b) cross-wind/torsional frequency ratio of 0.84

correlation $\rho[\ddot{x}, \ddot{y}_a]$ shown in Fig. 8a.

For reduced wind velocities lower than 10, the correlation between the cross-wind acceleration responses at point A and point B, $\rho[\ddot{y}_a, \ddot{y}_b]$, for all cases are highly correlated, as shown in Fig. 8b, which indicate a negligible effect of the torsional motion on the cross-wind acceleration responses of the building model. On the other hand, for reduced wind velocities higher than 10, the torsional motion of the building model is more dominant for Case 2 and Case 3 as the correlation $\rho[\ddot{y}_a, \ddot{y}_b]$ drops off from the value of 1.0. In addition, the lowest value of the correlation $\rho[\ddot{y}_a, \ddot{y}_b]$ of about 0.90 was observed at reduced wind velocities of about 17.5 and 12.5 for Case 2 and Case 3 respectively, which indicate similar effects of the torsional motion for both cases of cross-wind/torsional frequency ratios. Although the lowest value of correlation $\rho[\ddot{y}_a, \ddot{y}_b]$ for Case 2 and Case 3 occurred at different reduced wind velocities due to the different cross-wind/torsional frequency ratio, both of them occurred at $(U_{cr})_T = \bar{U}_H / (n_{z-z} \cdot D_y) \cong 10$, where n_{z-z} is the torsional natural frequency of the building model. Therefore, this reduced wind velocity is referred to as the critical reduced wind velocity for torsional motion. The response of the building model at this critical reduced wind velocity is expected to be dominated by the torsional motion due to the effect of resonance between the torsional natural frequency of the building model and the vortex shedding frequency. This effect is clearly demonstrated by the results from the analysis of response spectrum, which indicates a significant contribution of vibrational energy from the torsional motion in the cross-wind responses for Case 2 and Case 3 as shown in Figs. 9a and 9b respectively.

4. Wind-induced response of tall buildings with complex motion: buildings with eccentricity

For the incident wind normal to the wide face of the building model, characteristics of the normalised resultant standard deviation acceleration responses of the eccentric CAARC building model in the along-wind direction, $\sigma_{\ddot{x}} / (2\pi n_{y-y})^2 D_y$, and cross-wind direction, $\sigma_{\ddot{y}_a} / (2\pi n_{x-x})^2 D_y$, expressed as a function of reduced wind velocity, $U_r = \bar{U}_H / (n_{x-x} \cdot D_y)$, are presented in Figs. 10a and 10b respectively.

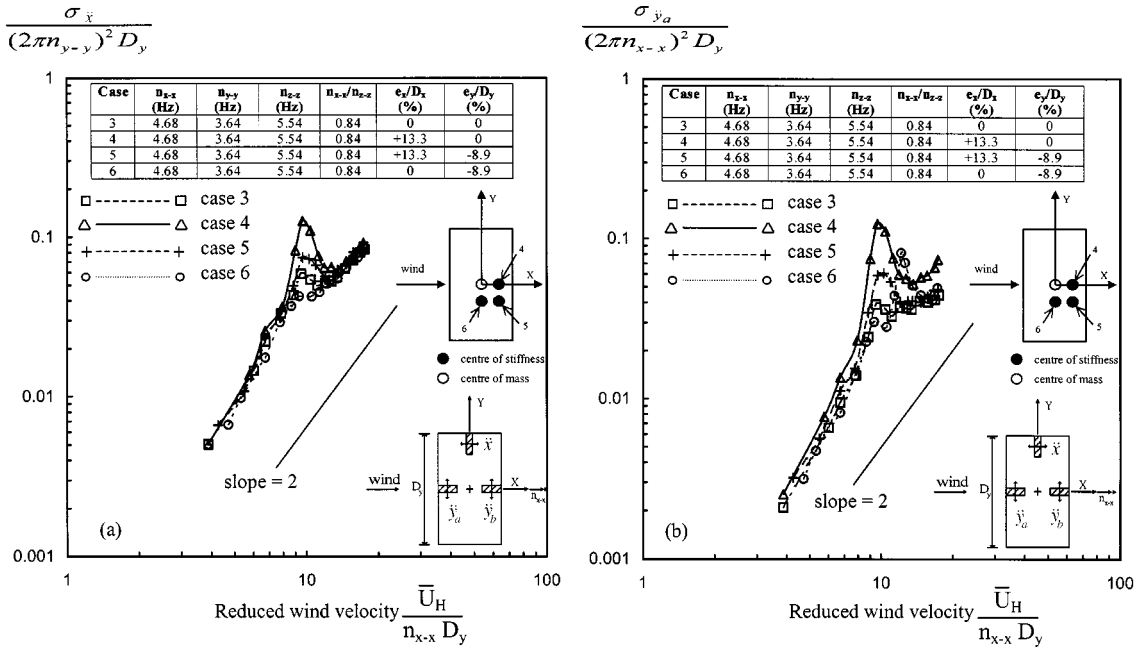


Fig. 10 Normalised resultant standard deviation acceleration responses at top of the CAARC building model as a function of reduced wind velocity for different eccentricities: (a) along-wind responses; (b) cross-wind responses

For reduced wind velocities ranging from 4 to 20, the eccentricity between centre of mass and centre of stiffness of the building model significantly affect the normalised resultant standard deviation along-wind and cross-wind acceleration responses, in particular at reduced wind velocities close to a critical value of 10. This effect of eccentricity was found to vary from case-to-case depending upon the location of the centre of stiffness.

4.1. Resultant along-wind and cross-wind acceleration responses of the CAARC building model for reduced wind velocities ranging from 4 to 8

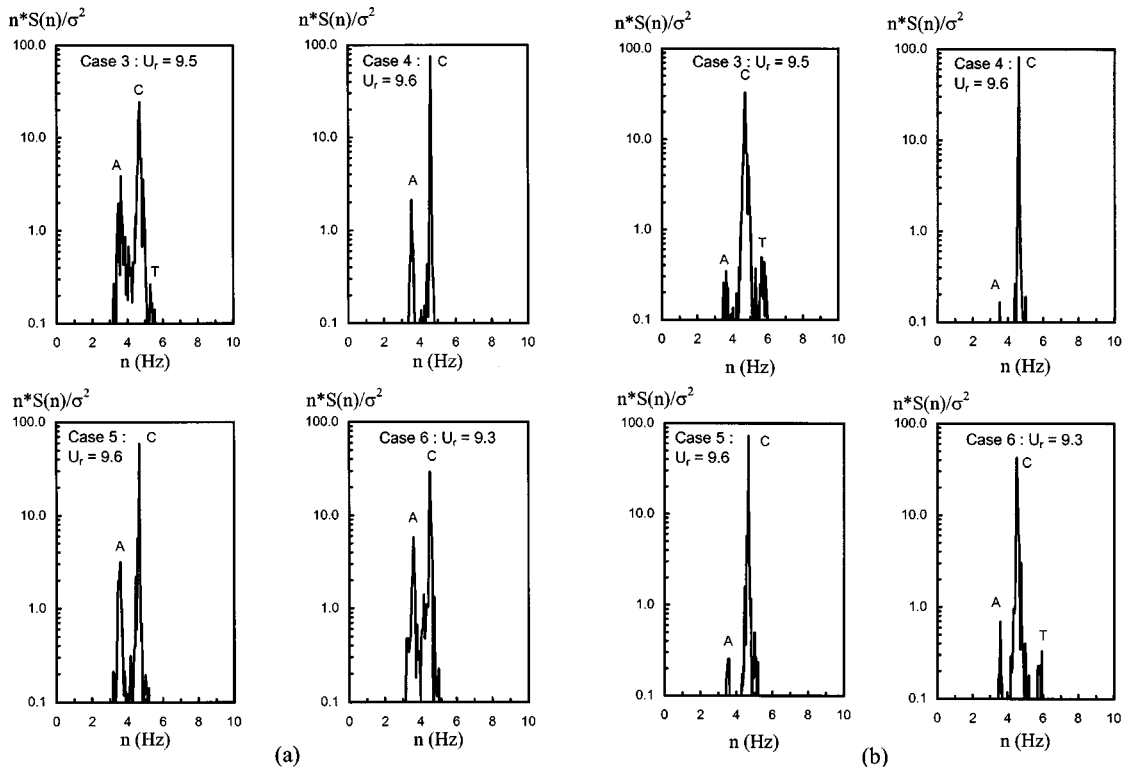
The eccentricity between centre of mass and centre of stiffness of the building model has little effects on the normalised resultant standard deviation along-wind responses for all eccentricity cases as shown in Fig. 10a. The results from the analysis of upcrossing frequency also suggested that the along-wind response process is a near normal distribution due to the well-known incident turbulent forcing mechanism.

For the CAARC building model with the cross-wind/torsional frequency ratio of 0.84, eccentricity between centre of mass and centre of stiffness can cause either an increase or a decrease in the normalised resultant standard deviation cross-wind response, depending upon the location of the centre of stiffness, as shown in Fig. 10b. With the centre of stiffness located at $e_x/D_x = 0.133$ down-wind, i.e., for Case 4, the normalised cross-wind response was amplified by up to 40% from the reference values of Case 3. On the other hand, for the building model Case 6 with the centre of stiffness located at $e_y/D_y = -0.089$ side-wind, the normalised cross-wind response was essentially

unchanged. The normalised cross-wind response for Case 5 was found to be between the responses for Case 4 and Case 6 as this case contains both eccentricities down-wind and side-wind. It was also found from the analysis of upcrossing frequency that the cross-wind response process was a near normally distributed process for all eccentricity cases. In addition, for reduced wind velocities ranging from 4 to 8, the vortex shedding process and the wake excitation mechanism remain the dominant excitation mechanism in the cross-wind direction even for tall buildings with coupled translational-torsional motion and with eccentricity between centre of mass and centre of stiffness.

4.2. Resultant along-wind and cross-wind acceleration responses of the CAARC building model for reduced wind velocities ranging from 8 to 12

For reduced wind velocities close to a critical value of 10, a significant increase in the normalised resultant standard deviation along-wind response by more than 100% and 25% was observed for Case 4 and Case 5 respectively, and a decrease by 20% was found for Case 6, as shown in Fig. 10a. This is thought to be related to a transfer of vibrational energy from the cross-wind oscillation through the torsional motion. This is readily illustrated by the results from the analysis of response spectrum, which indicate a significant contribution of vibrational energy from the cross-wind direction as shown in Fig. 11a. It is also evident that the contribution of vibrational energy from the



Note : A = Along-wind ; C = Cross-wind ; T = Torsion ; $U_r = U_H/n_x \cdot D_y$

Fig. 11 Acceleration response spectra of the CAARC building model for reduced wind velocities close to a critical value of 10 for different eccentricities: (a) along-wind responses; (b) cross-wind responses

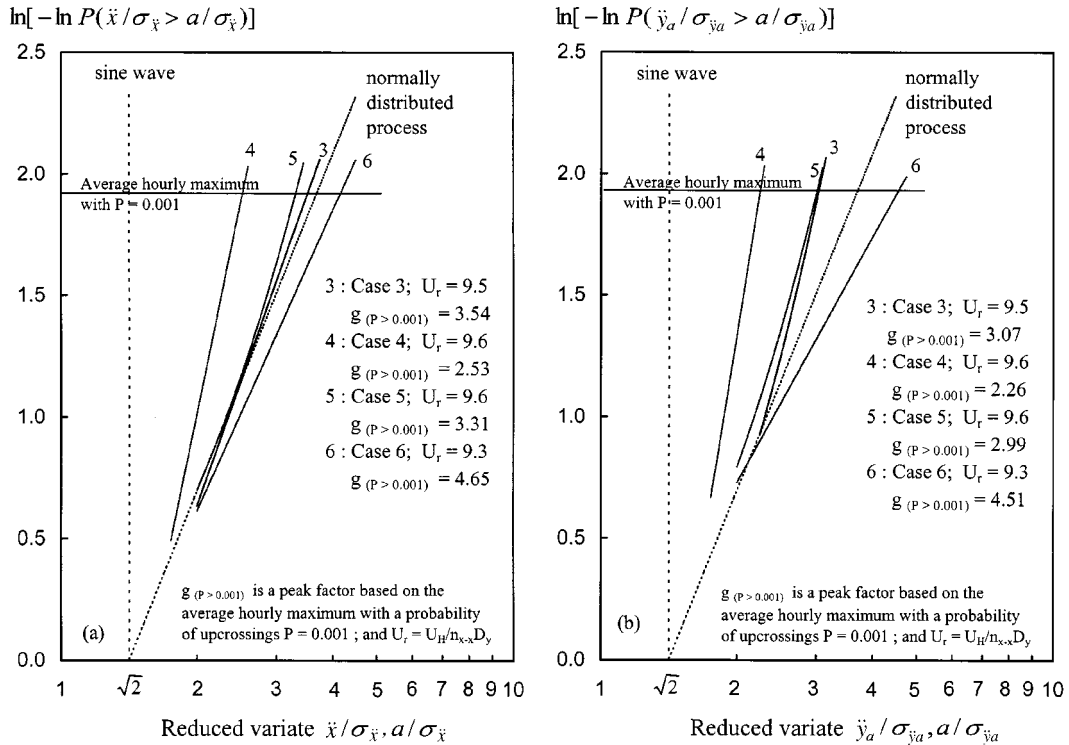


Fig. 12 Normalised upcrossing frequency of the CAARC building model for reduced wind velocities close to a critical value of 10 for different eccentricities: (a) along-wind responses; (b) cross-wind responses

along-wind motion for Case 6 is highest compared with the other cases. This is due to a higher translational component in the along-wind direction for the responses at point C caused by the effects of coupling between the translational and torsional vibration mode shapes, i.e., complex motion, as the centre of twist was shifted laterally side-wind. For Case 4, significant vibrational energy resulting from the amplitude-dependent excitation in the cross-wind direction is apparently transferred to the along-wind direction causing a significant increase in the along-wind response, as shown in Fig. 10a. In addition, a clear departure of the upcrossing frequency of the along-wind response from being normally distributed as shown in Fig. 12a, is believed to be caused by the effect of this energy transfer. However, when the centre of stiffness was located laterally side-wind, i.e., for Case 6, the effect of the energy transfer is less dominant, as the along-wind response process becomes a near normally distributed process, as shown in Fig. 12a.

For reduced wind velocities close to a critical value of 10, a considerable increase in the normalised cross-wind response by more than 200% for Case 4 and 50% for Case 5, and a decrease by 20% for Case 6, are evident as shown in Fig. 10b. These results highlight a significant impact of eccentricity between centre of mass and centre of stiffness on the amplitude-dependent effect caused by the vortex resonant process and the characteristic of the normalised cross-wind response of the building model. In general, for the building model with a cross-wind/torsional frequency ratio of 0.84, an eccentricity down-wind, i.e., for Case 4, tends to increase the normalised cross-wind response, and an eccentricity side-wind, i.e., for Case 6, tends to decrease the normalised cross-wind

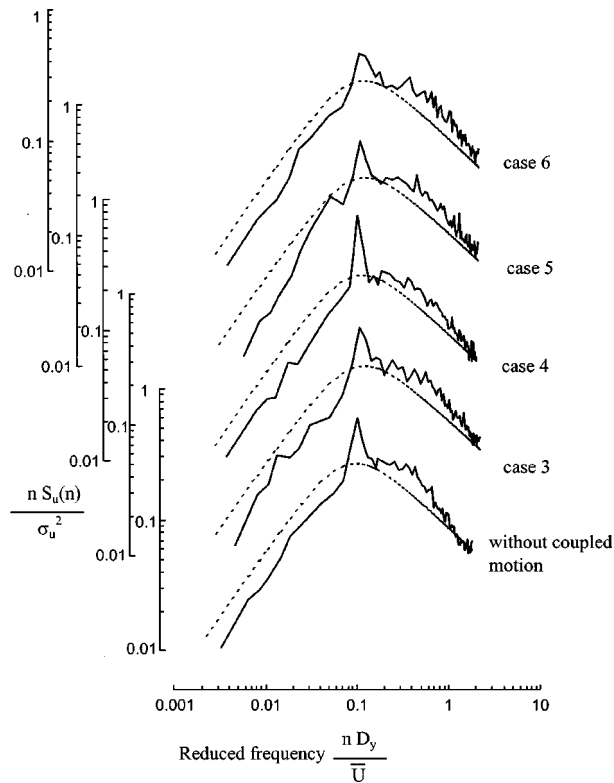


Fig. 13 Wake spectra of the CAARC building model at a reduced wind velocity of 9.65 (after Thepmongkorn and Kwok 1998)

response. In addition, the response for Case 6 exhibits a sharp decrease at reduced wind velocities close to a critical value of 10, but on the other hand a prominent peak in the normalised cross-wind response at a reduced wind velocity of about 12 is evident. This peak in the normalised cross-wind response is believed to be caused by the effect of resonance between the torsional natural frequency of the building model and the vortex shedding frequency; therefore, this reduced wind velocity is referred to as the critical reduced wind velocity for torsional motion.

Wake spectra of the CAARC building model with eccentricity between centre of mass and centre of stiffness are shown in Fig. 13. The wake spectra of the building model without torsional motion, and the longitudinal velocity spectrum of the upstream wind measured at top of the model, as seen by the dotted lines, are also shown in the figure for comparison. The wake spectra provide a reasonable representation of the energy available in the wake and assessment will be made mainly in terms of frequency distribution of this energy. It was found that the energy of velocity fluctuations in the wake is concentrated at a reduced frequency of about 0.1 for all cases. The peak of the wake spectra at the reduced frequency of 0.1 is consistent with the concentrated excitation energy associated with the vortex shedding process, which is the most common wind excitation mechanisms for tall buildings without coupled translational-torsional motion and with sharp edges. This characteristic has been widely reported by many researchers, e.g., Melbourne (1975), Bearman and Davies (1975), Kwok and Melbourne (1981), and Kwok *et al.* (1988). It is concluded that the vortex shedding process remains the main excitation mechanism in the cross-wind direction even for

tall buildings with coupled translational-torsional motion and with eccentricity between centre of mass and centre of stiffness.

The cross-wind response of the building model is dominated by the cross-wind motion, as indicated by the peaks at the cross-wind natural frequencies in the response spectra shown in Fig. 11b. The spectral peak for Case 4 indicates the significant amplitude-dependent effect resulting from the vortex resonant process, causing the peak in the normalised cross-wind response at reduced wind velocity close to a critical value of 10 as shown in Fig. 10b. This is confirmed by the result from the analysis of upcrossing frequency shown in Fig. 12b, which indicates a clear departure of the upcrossing frequency of the cross-wind response from a normally distributed process. On the other hand, when the centre of stiffness was located laterally side-wind, i.e., for Case 6, the response process is a near normal distribution. For Case 5, which contains both eccentricities down-wind and side-wind, the cross-wind response process is also essentially normally distributed.

4.3. Resultant along-wind and cross-wind acceleration responses of the CAARC building model for reduced wind velocities higher than 12

Eccentricity between centre of mass and centre of stiffness has a negligible effect on the normalised resultant standard deviation along-wind response of the building model as shown in Fig. 10a. The along-wind response process was also found to be normally distributed for all eccentricity cases.

In the normalised resultant standard deviation cross-wind response shown in Fig. 10b, the response for Case 4 was increased from the reference values of Case 3, while the response for Case 5 was essentially unchanged. In addition, beyond the peak at a reduced wind velocity of 12, the response for Case 6 sharply dropped and approached the response for Case 3. The cross-wind response process was found to be a near normally distributed process for all eccentricity cases due to the dominant wake excitation mechanism.

4.4. Significance of torsional motion from the analysis of correlation between response components

The correlation between the along-wind and cross-wind acceleration responses, $\rho[\ddot{x}, \ddot{y}_a]$, and correlation between the cross-wind acceleration responses at point A and point B, $\rho[\ddot{y}_a, \ddot{y}_b]$, are presented in Figs. 14a and 14b respectively.

For reduced wind velocities ranging from 4 to 8, the correlation between the along-wind and cross-wind acceleration responses, $\rho[\ddot{x}, \ddot{y}_a]$, for all eccentricity cases tend to increase as the mean wind speed increases, as shown in Fig. 14a. The negative values of the correlation $\rho[\ddot{x}, \ddot{y}_a]$ for all cases indicate a change in the phase lag between the along-wind and cross-wind motions due to changes in the ratio of frequencies between those responses as discussed in Section 3.4. For Case 4, the magnitude of the correlation $\rho[\ddot{x}, \ddot{y}_a]$ is generally higher than the correlation for other cases, in particular for reduced wind velocities close to a critical value of 10, where the highest correlation $\rho[\ddot{x}, \ddot{y}_a]$ of about -0.95 is observed. This is consistent with an enhanced transfer of vibrational energy from the cross-wind oscillation to the along-wind direction due to the eccentricity down-wind. For all eccentricity cases, the correlation $\rho[\ddot{x}, \ddot{y}_a]$ peaks at reduced wind velocities close to a critical value of 10 and tends to decrease as the mean wind speed increases and finally becomes constant for reduced wind velocities higher than approximately 15.

For reduced wind velocities lower than 10, the cross-wind acceleration responses at point A and

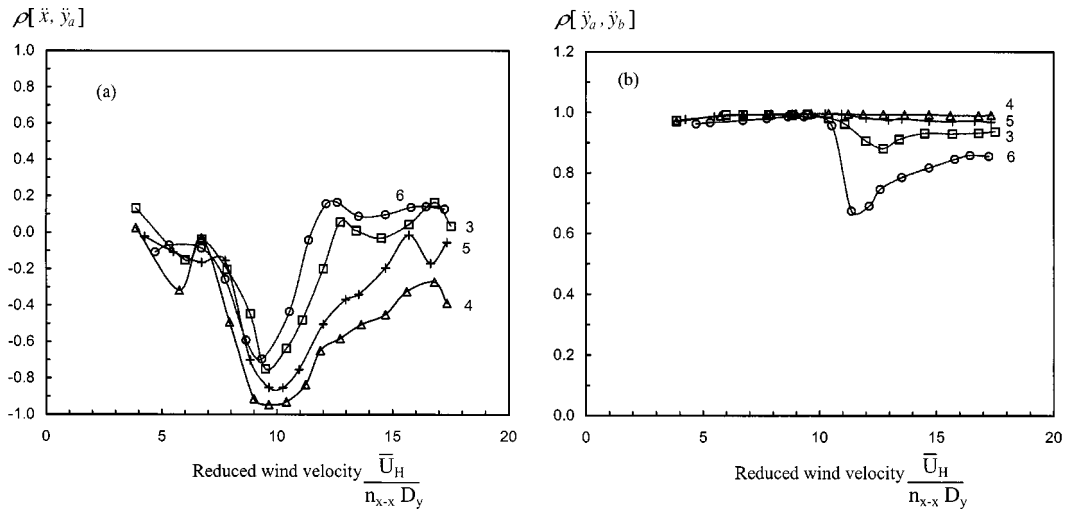
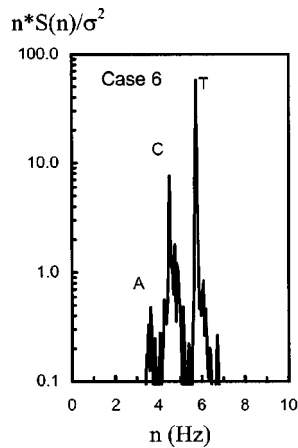


Fig. 14 Correlation between response components: (a) along-wind and cross-wind responses; (b) cross-wind responses at point A and point B



Note : A = Along-wind ; C = Cross-wind ; T = Torsion

Fig. 15 Cross-wind acceleration response spectra of the CAARC building model at the critical reduced wind velocity for torsional motion for the cross-wind/torsional frequency ratio of 0.84 and eccentricity side-wind

point B, $\rho[\ddot{y}_a, \ddot{y}_b]$, for all eccentricity cases are highly correlated, indicating a negligible effect of the torsional motion on the cross-wind responses, as shown in Fig. 14b. This appears to be independent of the eccentricity between centre of mass and centre of stiffness of the building model. For Case 4 and Case 5, the torsional motion also has a negligible effect on the cross-wind responses, for reduced wind velocities higher than 10, as seen by the very high correlation $\rho[\ddot{y}_a, \ddot{y}_b]$ for both cases. However, when the centre of stiffness was located laterally side-wind (Case 6), the effect of torsional motion is significant as the correlation $\rho[\ddot{y}_a, \ddot{y}_b]$ drops sharply to the lowest value at a reduced wind velocity of about 12. This is due to the effect of resonance between the torsional natural frequency of the building model and the vortex shedding frequency, hence the building is

operating at the critical reduced wind velocity for torsional motion, $(U_{cr})_T$. The cross-wind response spectrum for Case 6 at this critical reduced wind velocity for torsional motion, $(U_{cr})_T$ is given in Fig. 15, which clearly demonstrates the significant contribution of vibrational energy from the torsional motion.

5. Conclusions

Wind tunnel aeroelastic model tests of the CAARC standard tall building using a three-degree-of-freedom BHA model were performed. The experimental results highlighted the significant effects of coupled translational-torsional motion, and eccentricity between centre of mass and centre of stiffness, on both the normalised resultant standard deviation along-wind and cross-wind acceleration responses for reduced wind velocities ranging from 4 to 20.

For the CAARC building model with a cross-wind/torsional frequency ratio of 0.60, coupled translational-torsional motion has a negligible effect on the normalised resultant standard deviation along-wind acceleration response for the range of reduced wind velocities tested. However, an increase in the normalised along-wind response due to a transfer of vibrational energy from cross-wind oscillations was observed at reduced wind velocities close to a critical value of 10. On the other hand, when the cross-wind/torsional frequency ratio was 0.84, a significant increase in the normalised along-wind acceleration response is evident, especially at reduced wind velocities close to a critical value of 10, due to an enhanced energy transferred from the cross-wind direction. These results highlight the significant effect of the cross-wind/torsional frequency ratio on the transfer of vibrational energy from the cross-wind oscillations, which can amplify the normalised along-wind response by more than 100%.

At reduced wind velocities close to a critical value of 10, a significant reduction in the normalised resultant standard deviation cross-wind acceleration response by more than 50% was observed for both cases of cross-wind/torsional frequency ratios. Coupled translational-torsional motion evidently alters the amplitude-dependent effect caused by the vortex resonant process and significantly reduces the normalised cross-wind response at this reduced wind velocities range. Furthermore, this effect of coupled translational-torsional motion appears to be independent of the cross-wind/torsional frequency ratio.

Coupled translational-torsional motion has a negligible effect on the excitation associated with the vortex shedding process, hence the vortex shedding process remains the dominant excitation mechanism in the cross-wind direction. In addition, the contribution from the torsional motion to the cross-wind response was found to be greatly amplified by the resonant mechanism resulting from the coincidence between the torsional natural frequency of the building model and the vortex shedding frequency.

When the centre of stiffness of the building model was located laterally down-wind from the centre of mass, an increase in the normalised resultant standard deviation cross-wind response is observed. In particular, a considerable increase at reduced wind velocities close to a critical value of 10 due to the amplitude-dependent effect resulting from the vortex resonant process is evident. In addition, the significant increase in the normalised resultant standard deviation along-wind response by 40% due to an apparent transfer of vibrational energy from the cross-wind oscillation is observed for reduced wind velocities close to a critical value of 10.

When the centre of stiffness was located laterally side-wind from the centre of mass, the vortex shedding process and wake excitation remain the dominant excitation mechanisms in the cross-wind

direction. However, for reduced wind velocities close to a critical value of 10, the amplitude-dependent excitation caused by the vortex resonant process was not evident and this resulted in a decrease in the normalised resultant standard deviation cross-wind response. Furthermore, when the vortex shedding frequency coincides with the torsional natural frequency of the building model, that is at the critical reduced wind velocity for torsional motion, the normalised cross-wind response of the building model was found to be greatly amplified by the torsional resonant mechanism.

References

- Bearman, P.W. and Davies, M.E. (1975), "The flow about oscillating bluff structures", *Proc. of 4th Int. Conf. Wind Effects on Buildings and Struct.*, Heathrow, UK, 285-295.
- Hart, G.C., DiJulio, R.M.Jr. and Lew M. (1975), "Torsional response of high-rise buildings", *J. Struct. Div.*, ASCE, **101**(ST2), 397-416.
- Kareem, A. (1985), "Lateral-torsional motion of tall buildings to wind loads", *J. Struct. Eng.*, ASCE, **111**(11), 2479-2496.
- Kwok, K.C.S. (1977), "Cross-wind response of structures due to displacement dependent excitations", Thesis presented to the Department of Mechanical Engineering, Monash University, Australia, in fulfilment for the degree of Doctor of Philosophy.
- Kwok, K.C.S. and Melbourne, W.H. (1981), "Wind-induced lock-in excitation of tall structures", *J. Struct. Div.*, ASCE, **107**(ST1), 57-72.
- Kwok, K.C.S., Wilhelm, P.A. and Wilkie, B.G. (1988), "Effect of edge configuration on wind-induced response of tall buildings", *Eng. Struct.*, **10**, 135-140.
- Kwok, K.C.S., Lakshmanan, N. and Donovan, P.F. (1994), "Development of a special base hinge assembly for stick models", Report PROJ.UNDP/AND/91/011, Structural Engineering Research Centre, Madras, India.
- Melbourne, W.H. (1974), "Response of a slender tower to wind excitation", *Proc. 5th Australasian Conf. on Hydraulics and Fluid Mechanics*, University of Canterbury, New Zealand, 251-257.
- Melbourne, W.H. (1975), "Cross-wind response of structures to wind action", *Proc. 4th Int. Conf. on Wind Effects on Buildings and Struct.*, Heathrow, UK, 343-358.
- Melbourne, W.H. (1977), "Probability distributions associated with the wind loading of structures", *Civil Engineering Transactions*, The Institution of Engineers, Australia, **CE 19**(1), 58-67.
- Patrickson, C.P. and Friedmann, P.P. (1979), "Deterministic torsional building response to winds", *J. Struct. Div.*, ASCE, **105**(ST12), 2621-2637.
- Saunders, J.W. (1974), "Wind excitation of tall buildings with particular reference to the cross-wind motion of tall buildings of constant rectangular cross-section", Thesis presented to the Department of Mechanical Engineering, Monash University, Australia, in fulfilment for the degree of Doctor of Philosophy.
- Standards Australia (1989), SAA Loading Code Part 2: Wind Loads, AS1170.2-1989.
- Tallin, A. and Ellingwood, B. (1985), "Wind induced lateral-torsional motion of buildings", *J. Struct. Eng.*, ASCE, **111**(10), 2197-2213.
- Thepmongkorn, S. and Kwok, K.C.S. (1998), "Wind-induced coupled translational-torsional motion of tall buildings", *Wind and Structures*, **1**(1), 43-57.
- Thepmongkorn, S., Kwok, K.C.S. and Lakshmanan, N. (1999), "A two-degree-of-freedom base hinged aeroelastic (BHA) model for response predictions", *J. Wind Eng. Ind. Aerod.*, **83**, 171-181.
- Yip, D.Y.N. (1995), "Wind-induced dynamic response of tall buildings with coupled 3D modes of vibration", Thesis presented to the Department of Mechanical Engineering, the University of Auckland, New Zealand, in fulfilment for the degree of Doctor of Philosophy.
- Yip, D.Y.N. and Flay, R.G.J. (1995), "A new force balance data analysis method for wind response predictions of tall buildings", *J. Wind Eng. Ind. Aerod.*, **54/55**, 457-471.
- Yoshie, R., Kawai, H., Shimura, M. and Wei, R. (1997), "A study on wind-induced vibration of super high rise building by multi-degree-of-freedom model", *J. Wind Eng. Ind. Aerod.*, **69-71**, 745-755.